ISSN 2181-1369

# IRRIGATSIYA va MELIORATSIYA

№1(31).2023

*Journal of Irrigation and Melioration*

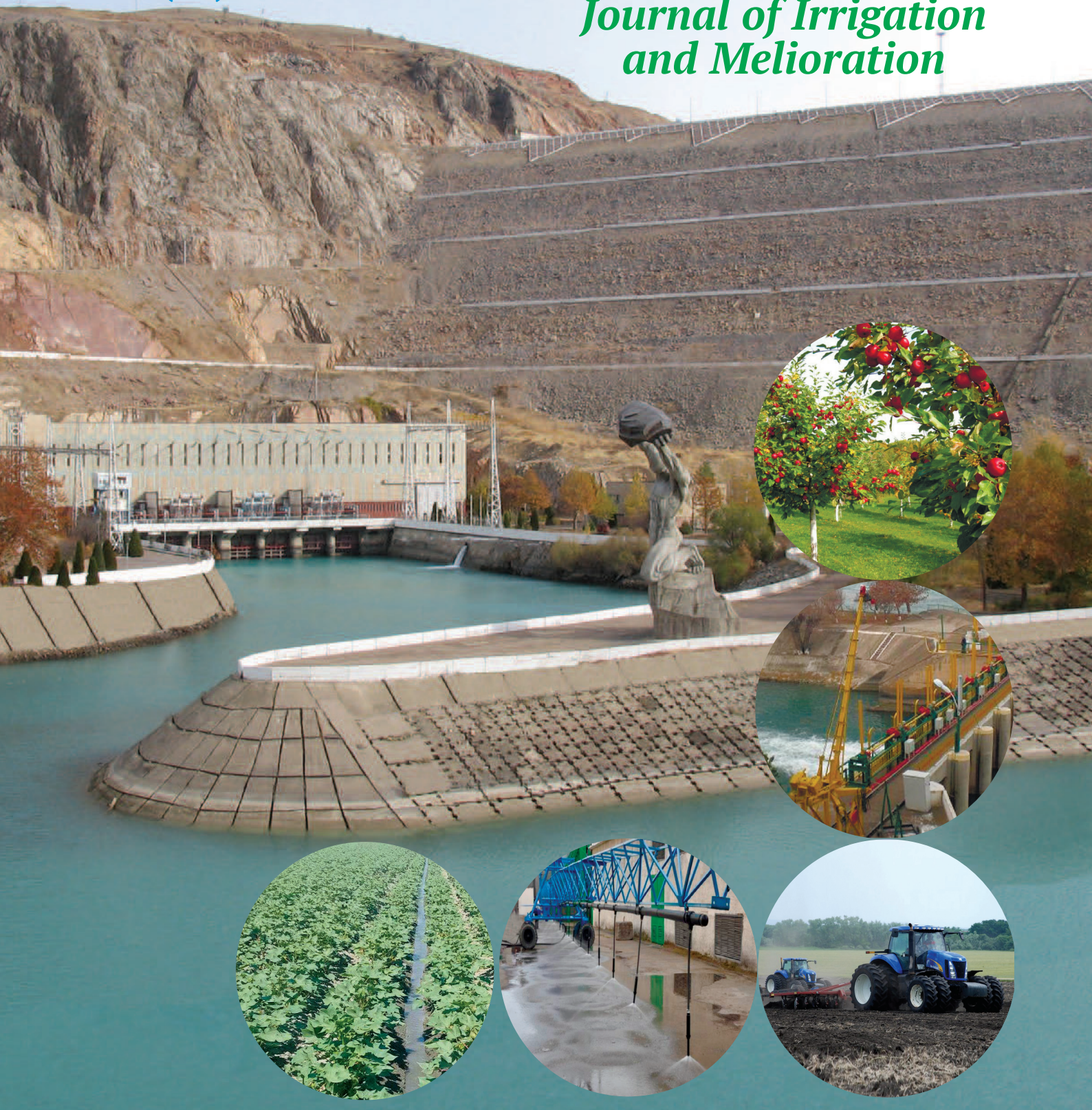

## ИРРИГАЦИЯ ВА МЕЛИОРАЦИЯ



## ГИДРОТЕХНИКА ИНШООТЛАРИ ВА НАСОС СТАНЦИЯЛАР



## ҚИШЛОҚ ХЎЖАЛИГИНИ МЕХАНИЗАЦИЯЛАШ



## ҚИШЛОҚ ХЎЖАЛИГИНИ ЭЛЕКТРЛАШТИРИШ ВА АВТОМАТЛАШТИРИШ



## СУВ ХЎЖАЛИГИ СОҲАСИ УЧУН КАДРЛАР ТАЙЁРЛАШ

*UDC: 539.3*

# DEVELOPMENT AND RESEARCH OF THE METHOD OF STATIC SYSTEMS IDENTIFICATION BY HYSTERESIS

***B.A.Khudayarov – DSc, professor, F.Zh.Turaev – senior teacher,***
***"Tashkent Institute of Irrigation and Agricultural Mechanization Engineers" National Research University***

**Abstract**

The paper considers methods for constructing and numerical realization of a hysteresis model for engineering systems. Mathematical models based on the analytical representation of the hysteresis characteristics of linear systems obtained by specifying piecewise linear signals at their input with different velocities of both signs on linear sections are proposed. For a more accurate description of the hysteresis characteristics of static systems that actually occur in practice, in a number of cases, differential equations of higher order are used, in particular, equations of the second order. The use of differential equations of higher order makes it possible to simulate cyclically unstable hysteresis, when the shape and slope of the hysteresis curves can change from a cycle to a number of cycles. For some systems, this process ends after a certain number of cycles (there is a so-called transient process in the phenomenon of hysteresis, in electrical engineering, it is called accommodation in relation to magnetic elements), for other systems this process of cyclic instability of hysteresis can be observed for any length of time. Methods for identifying static objects by hysteresis were developed and investigated.

**Key words:** hysteresis, integral model, Rayleigh-Masing principle, differential equations, numerical model, input signal.

# STATIK TIZIMLARNI HISTEREZIS ORQALI ANIQLASH USULINI ISHLAB CHIQISH VA TADQIQ QILISH

***B.A.Xudayarov – t.f.d, professor, F.J.Turayev – katta oʻqituvchi,***
***"Toshkent irrigatsiya va qishloq xoʻjaligini mexanizatsiyalash muhandislari instituti" milliy tadqiqot universiteti***

**Annotatsiya**

Maqolada texnik tizimlarning histerezis modelini yaratish va raqamli amalga oshirish usullari koʻrib chiqilgan. Matematik modellar chiziqli kesmalarda ikkala belgining turli tezligiga ega boʻlakli chiziqli signallarga kirishini oʻrnatish orqali olingan chiziqli tizimlarning histerezis xususiyatlarini analitik tasvirlash asosida taklif etiladi. Amalda haqiqatda sodir boʻladigan statik tizimlarning histerezis xususiyatlarini aniqroq tavsiflash uchun ba'zi hollarda yuqori tartibli differensial tenglamalar, xususan, ikkinchi tartibli tenglamalar qoʻllaniladi. Yuqori tartibli differensial tenglamalardan foydalanish, histerezis egri chiziqlarning shakli va qiyaligi sikldan siklga oʻzgarishi mumkin boʻlgan holda, siklik beqaror histerezisni modellashtirishga imkon beradi. Ba'zi tizimlar uchun bu jarayon ma'lum miqdordagi sikllardan soʻng tugaydi (histerezis hodisasida vaqtinchalikjarayon deb ataladigan narsa bor, elektrotexnikada u magnit elementlarga nisbatan akkomodatsiya deb ataladi), boshqa tizimlar uchun bu siklik histerezis jarayoni beqarorlik har qanday vaqt davomida kuzatilishi mumkin. Statik obektlarni histerezis orqali aniqlash usullari ishlab chiqilgan va organilgan.

**Tayanch soʻzlar:** histerezis, integral model, Reyl-Masing printsipi, differentsial tenglamalar, sonli model, kirish signali.

# РАЗРАБОТКА И ИССЛЕДОВАНИЕ МЕТОДА ИДЕНТИФИКА ЦИИ СТАТИЧЕСКИХ СИСТЕМ ПО ГИСТЕРЕЗИСУ

***Б.А.Худаяров – д.т.н., профессор, Ф.Ж.Тураев – старший преподаватель,***
***Национальный исследовательский университет «Ташкентский институт инженеров ирригации и механизации сельского хозяйства»***

**Аннотация**

В статье рассмотрены методы построения и численной реализации гистерезисной модели технических систем. Предложены математические модели, основанные на аналитическом представлении гистерезисных характеристик линейных систем, полученных путем задания на их вход кусочно-линейных сигналов с различными скоростями обоих знаков на линейных участках. Для более точного описания гистерезисных характеристик статических систем, реально встречающихся на практике, в ряде случаев используют дифференциальные уравнения более высокого порядка, в частности уравнения второго порядка, использование которых, позволяет моделировать циклически неустойчивый гистерезис, когда форма и наклон кривых гистерезиса могут меняться от цикла к числу циклов. Для одних систем этот процесс заканчивается через определенное число циклов (существует так называемый переходный процесс в явлении гистерезиса, в электротехнике он называется аккомодацией по отношению к магнитным элементам), для других систем этот процесс циклической нестабильности гистерезиса может наблюдаться в течение любого промежутка времени. Разработаны и исследованы методы идентификации статических объектов по гистерезису.

**Ключевые слова:** гистерезис, интегральная модель, принцип Рэлея-Мазинга, дифференциальные уравнения, численная модель, входной сигнал.

**Introduction.** Many systems used in practice include various sources of energy dissipation (nodes with external and internal friction, ferromagnets, ferroelectric capacitors, and others), switching devices and nonlinear elements with an ambiguous static characteristic. For such systems, called hysteresis systems, with an arbitrary law of variation of the input coordinate $X(t)$ , the motion of the representing point will have a complex hysteresis nature, when a finite or infinite set of values of the output coordinate $Y$ corresponds to one value of $X$.

Hysteresis systems are called static systems in the range $|X|<X_0$, where $X_0$ is a certain threshold value of speed, at exceeding which the speed affects the course of the hysteresis curves, if the shape and slope of the branches of the hysteresis loops do not depend on the value in the indicated range of speeds; at that, at the turning points at which the sign changes to the opposite sign, an acute-angled shape of the loop (tips) with a break of the first kind is observed.

Since the second half of the 19th century, when the phenomenon of hysteresis was discovered, attempts have been made to analytically describe static hysteresis in order to use the obtained formulas and equations in calculating electrical machines, mechanical structures, buildings, etc.

The Rayleigh-Masing mathematical model can be physically substantiated based on the assumption that any system with hysteresis can be considered as a set of a large number of ideal elastic-plastic elements with different values of the yield stress. For example, a polycrystalline body is represented as consisting of a significant number of individual conditional grains, arbitrarily oriented relative to the direction of force action. Some mechanical characteristics of a conditional grain, as well as its relationship with neighboring grains, can be postulated. S.P.Tymoshenko [1] proposed this approach back in 1930. However, for a long time, it did not attract much attention from researchers. Apparently, this is due to the fact that this approach of a "continual" character frightened off researchers by the seeming difficulty of deriving the relationship between force and displacement.

In 1944, A.Yu. Ishlinsky [2] obtained the initial stress-strain diagram of a specimen of a given material, and the diagrams of its subsequent alternating loading, by a static method based on the above-described "continual" approach to the problem of hysteresis of solids.

After this study, a number of articles by other authors were published [3. 4. 5. 6], in which the ideas of S.P.Timoshenko and A.Yu.Ishlinsky were further developed. In the articles mentioned above, it has been convincingly shown how a relatively simple hysteresis model can be constructed using the "continual" approach, reflecting the essential aspects of this phenomenon; this model can be applied to study oscillatory processes in systems with a hysteresis.

Many crystalline materials such as ferromagnets, ferroelectrics and ferroelastics are characterized by hysteresis, i.e. by ambiguous relationship between input and output magnetic, electrical and mechanical quantities, respectively [7].

In [8], a mathematical model of hysteresis of the water-holding capacity of soil was proposed. The mathematical model was based on physical concepts of the structure and capillary properties of the soil pore space. The mathematical model of the hysteresis water-holding capacity of soil makes it possible to assess the hydrophysical characteristics of soil, used in the design of hydro-technical structures, as well as in the calculation of irrigation norms. The estimates obtained in the framework of computational experiments using this model contribute to an increase in the efficiency of studying the hydrological conditions of the territory of hydro-technical structures when performing pre-design engineering surveys.

The study in [9] proposed a model that depends on the wetting angle in an incremental form to reproduce the behavior of soil-water hysteresis. A proportional distribution function is proposed for dividing the suction increments into two parts, one of which is designed to change the effective degree of saturation, and the other - to change the contact angle. The proposed hysteresis model contains only four parameters that can be conveniently calibrated using the main branch of drying and the scanning curve of wetting. The model is confirmed by comparison with experimental data.

In [10], the mechanisms of hysteresis in porous media were investigated and a numerical model for unfrozen liquid was developed, which is able to describe the phenomenon of hysteresis in freezing and thawing cycles. The authors presents a coupled finite element model as a basis for numerical modeling of fluid flow and heat transfer in partially frozen porous media.

A model of pore expansion and contraction hysteresis caused by hydraulic loading was proposed in [11]. The physical mechanism of expansion and contraction was revealed through a microscopic model based on the fundamental principles of the axis displacement technique. In addition, the pore radius of the porous medium is redefined to determine the upper and lower boundaries of the pore expansion and contraction. Differential hysteresis equations are constructed in combination with a two-parameter equation. The numerical results are in good agreement with the experimental data.

In [12], the hydraulic hysteresis in unsaturated soils was studied, and the energy dissipation associated with the elastoplastic process and the main processes of wetting and drying were derived. Based on the hysteresis curve of water retention for deformable soils, a combined hydromechanical model was formulated. Experimental tests were carried out to verify the proposed hysteresis model.

[13] presents a general algorithm for estimating the damping coefficient, modeled by any constitutive model, based on the registered behavior in the three-dimensional "stress-strain" space.

A simple phenomenological approach to modeling the soil-water characteristic hysteresis curve following arbitrary wetting/drying cycles was presented in [14].

In [15], a model of water retention was proposed, depending on the void ratio, taking into account the effect of hydraulic hysteresis. Structural degradation was modeled using an approach to strain strengthening, taking into account the effect of the stress magnitudes and accumulated plastic strain on the degradation process.

A surface model for describing the stress-strain relationship in unsaturated soil with constant matrix suction was proposed in [16]. Strain rates are introduced to account for the effect of cyclic loading history. The movable center image rule is used to describe the hysteresis characteristics of the dynamic stress-strain curve during the unloading process.

**Models and methods**

***Integral model of the first order of static hysteresis***

In one of the simplest cases, the field of hysteresis curves (hysteresis characteristic) of a static system can be represented as consisting of two differently oriented families of curves (plotted in Fig. 1 by a dotted line) fixed on the $XOY$ plane:

a) a family of curves along which the motion of the representing point occurs at $\dot{x} > 0$ (a family of load curves);

b) a family of curves along which the motion of the representing point occurs at $\dot{x} < 0$ (a family of load curves).

At $\dot{x} = 0$ the system is stationary (values of $X$ and $Y$ are fixed). When the sign of velocity $\dot{X}$ changes at some point $M_0(x_0, y_0)$ of the $XOY$ plane, the transition from the curve of one family to the curve of another family occurs passing through this point. In this case, the branches of the hysteresis cycle (shown in Fig. 1 by solid curves) obtained with an arbitrary law of variation $x(t)$ (at the bottom of Fig. 1) are located on the corresponding curves of both families.

The paper considers static hysteresis, which, as noted above, is characterized by the independence of the course of the curves from the velocity of disturbing effect on the system. Using this, we can represent the static hysteresis of the spatial type in three-dimensional space $XOY\dot{X}$ as a set of two families of integral surfaces of the cylindrical type, the generatrix of which with the plane $\dot{x} = const$ leads to the same pattern of plane hysteresis, as mentioned above. The $MNPQS$ phase trajectory located on one of the surfaces corresponding to $\dot{x} > 0$ is projected into one of the loading curves on the $XOY$ plane; along the phase trajectory, velocity $\dot{x}$ can be of any value, but with a positive sign. A similar situation is observed with any phase trajectory located on one of the integral planes at $\dot{x} < 0$. So in a visual spatial form, static hysteresis is presented in one of its simplest forms (Fig. 2).

Mathematically, each of the families of hysteresis curves shown in Fig. 1 is considered as a family of integral curves in domain $D$ of the $XOY$ plane, which is a solution to a differential equation of the first order, a nonlinear one, in the general case.

It is known that for a differential equation of the first order [1]

$$\frac{dy}{dx} = f(x, y) \tag{1}$$

where is defined in domain $D$ of the $XOY$ plane and is continuous in it together with its partial arbitrary with respect to $Y$ (by the condition of the Cauchy theorem on the existence and uniqueness of the solution to equation (1), the general solution is represented as some function

$$y = \phi(x, c) \tag{2}$$

with one arbitrary constant c.

Geometrically, this solution is represented in domain $D$ as a family of integral curves, with each individual integral curve corresponding to its own definite value of c (Fig. 3). This value of $c$ is determined by setting in (3) the coordinates of the point through which the given integral curve passes. Moreover, no matter what point $M_0(x_0, y_0)$ in domain $D$ we take, if the Cauchy condition is satisfied, only one integral curve will pass through it. In accordance with what has been stated from the theory of first-order differential equations, the hysteresis characteristic of a static system is described by functional relations with arbitrary constants $c_1$ and $c_2$ :

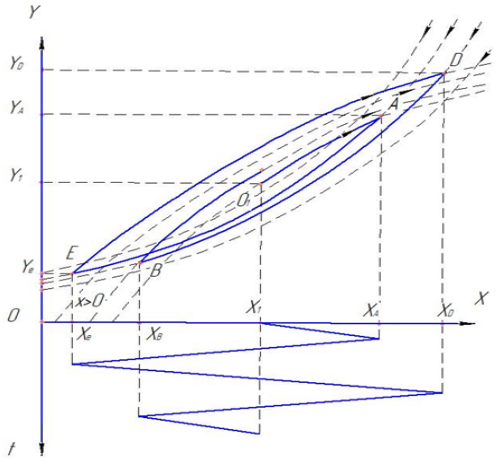


***Figure 1. Hysteresis curves***

$$y = \begin{cases} \varphi_1(x_1 c_1), \dot{x} > 0; \\ \varphi_2(x_2 c_2), \dot{x} < 0 \end{cases} \tag{3}$$

where: $\varphi_1$ describes a family of hysteresis curves at $\dot{x} > 0$ ; and $\varphi_2$ describes a family of hysteresis curves at $\dot{x} < 0$ ; as mentioned above, both of these families represent the hysteresis characteristic (hysteresis field) of a static object.

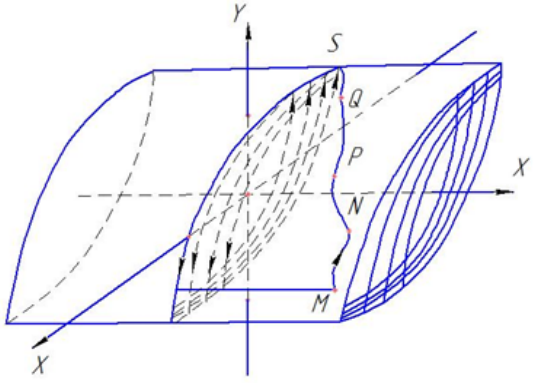


***Figure 2. Static hysteresis***

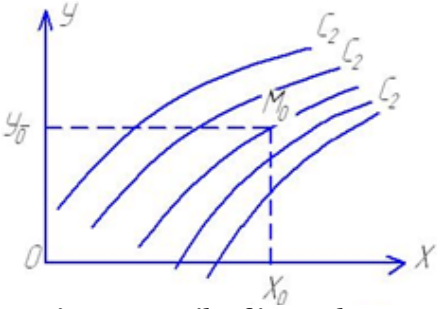


***Figure 3. Family of integral curves***

When setting an arbitrary law of variation (at the bottom of Fig. 1), the process of calculating the hysteresis cycle (shown in Fig. 1 by solid lines) based on relations (3) is realized as follows. At those points of the working field of the sample (in Fig. 1, points $O_1, A, B, C, Д, E$), at which the sign of velocity $\dot{x}$ (turning points) changes, the coordinates $X$, $Y$ are stored. These values of coordinates, depending on sign of $\dot{x}$ , are substituted into the first or second relation (3), as a result of which a specific value of an arbitrary constant $C_i (i = 1, 2)$ is

determined and, accordingly, a specific functional expression of the curve $y = \varphi_i(x, c_i)$, along which the movement from a given point occurs. At the turning points, the Cauchy problem known in the theory of first-order differential equations should be solved. If the solution to this problem is unambiguous, from this or any other turning point the movement will be performed only along one curve. This can be achieved by appropriate selection of functions $\varphi_1$ and $\varphi_2$.

In Fig. 4, a hysteresis loop calculated from relations (3) is shown by a harmonic law of variation $x(t)$ (a similar result is obtained by any other periodic law $x(t)$, as long as the sign of $\dot{x}$ does not change in every quarter of the period). It can be seen that the loop does not close after the first period. Moreover, the loop does not close after three or four periods and even more; theoretically it should close only after an infinite number of periods. This phenomenon is due to the fact that in the last quarter of the period the movement of the representing point occurs along an ascending integral curve located above the integral curve along which the movement was performed from the initial point $O_1$.

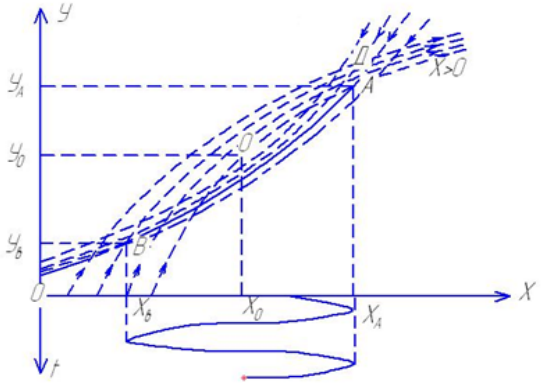


***Figure 4. Hysteresis loop***

Differentiating each of the relations (3) by $x$ and eliminating arbitrary constants $C_1$ and $C_2$, we obtain the following system of differential equations:

$$\frac{dy}{dx} = \begin{cases} f_1(x, y), \dot{x} > 0 \\ f_2(x, y), \dot{x} < 0 \end{cases} \quad (4)$$

the solution of which is the dependence $y(x)$ from expression (3).

When calculating an arbitrary hysteresis cycle using these equations, the coordinates of the points at which the velocity sign changes are used as initial conditions for the corresponding differential equation to which the transition is made.

The proposed models (3) and (4) make it possible to calculate (in manual way or using computers) arbitrary hysteresis cycles, including families of hysteresis loops at different amplitudes of $A$, at any point $M_0(x_0, y_0)$ (arbitrary asymmetry of the cycle) of the hysteresis cycle of the system.

The proposed integral hysteresis model made it possible to achieve not only qualitative, but also quantitative conformity of the calculated hysteresis cycles with the experimental ones. As far as is known, until now, in the theory of mechanical and electrical hysteresis, there were no models that satisfied these requirements.

An integral model of hysteresis characteristics, presented in a functional form (3), and a differential model (4) are suitable for calculating systems on computers. In the latter case, the solution of differential equations occurs continuously in time; in equations (4), considering the arbitrary nature of variation in $x(t)$, it is necessary to proceed to differentiation by $t$:

$$\frac{dy}{dt} = \begin{cases} f_1(x, y)\frac{dx}{dt}, \dot{x} > 0; \\ f_2(x, y)\frac{dx}{dt}, \dot{x} < 0. \end{cases} \quad (5)$$

Using relation:

$$\frac{dy}{dx} = \frac{dy}{dt} \Big/ \frac{dx}{dt}$$

it is not difficult to pass from equations (5) to an integral operator, if we perform the appropriate integration over $t$:

$$y = \int_0^t R_0[x(\tau), y(\tau)]\dot{x}(\tau)d\tau \quad (6)$$

where:

$$R_0[x(\tau), y(\tau)] = \begin{cases} f_1[x(\tau), y(\tau)], \dot{x} > 0; \\ f_2[x(\tau), y(\tau)], \dot{x} < 0, \end{cases} \quad (7)$$

is the kernel of the integral transformation (6).

When studying the oscillations of a system with one degree of freedom, the classical equation of oscillations:

$$\frac{d^2x}{dt^2} + \omega_0^2 y(x) = f_0(t) \quad (8)$$

is solved together with either functional expressions (3) or with differential equations (4) or (5). The disturbing force $f_0(t)$ can change by an arbitrary law, including a harmonic one.

In the case of an invertible system, the hysteresis characteristic are described by the following functional relationships:

$$x = \begin{cases} \Phi_1(y, c_1), \dot{y} > 0; \\ \Phi_2(y, c_2), \dot{y} < 0, \end{cases} \quad (9)$$

which are solutions of differential equations:

$$\frac{dx}{dt} = \begin{cases} F_1(x, y)\frac{dy}{dt}, \dot{y} > 0; \\ F_2(x, y)\frac{dy}{dt}, \dot{y} < 0, \end{cases} \quad (10)$$

where: $\Phi_1$ and $\Phi_2$ are functions invertible to functions $\varphi_1$ and $\varphi_2$ from relations (3).

For an invertible system, the integral operator (6) reverts into a nonlinear integral equation:

$$\int_0^t K_c[x(\tau), y(t)]\dot{y}(\tau)d\tau = x(t) \quad (11)$$

***On the application of a first-order integral model in calculating arbitrary hysteresis cycles***

The principle of calculating an arbitrary hysteresis cycle using the new integral model described in the previous section can be embedded into a computer program. At the same time, attention should be paid to the accuracy of calculating the turning point (the loop top). Since, for a given law $x(t)$, the computer calculates the branches of the hysteresis cycle with a step $\Delta t_0$, the accuracy of calculating the loop top is thus related to the accuracy of calculating the extremum of function $x(t)$. The program provides for the calculation of the extrema of this function with a given accuracy $\varepsilon_m$. If, as indicated in Fig. 5, the error in calculating the extremum exceeds $\varepsilon_m$, there will be a retreat two steps back and the given step is split by two, that is, there is a new step $\Delta t_0/2$. Backtracking and step splitting stop when the specified accuracy is reached.

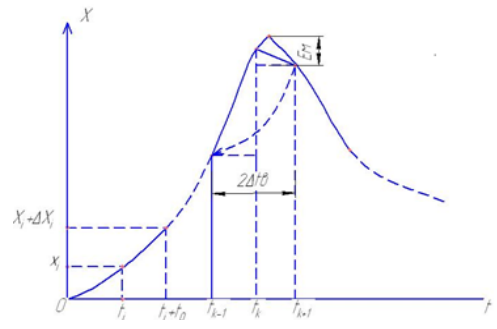

*Figure 5. Loop tops*

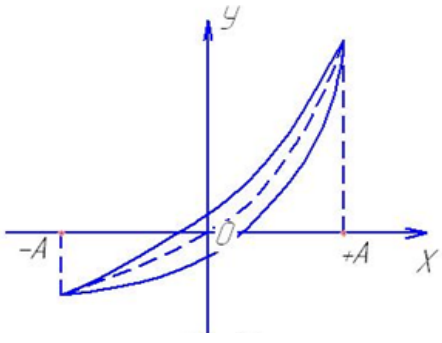

*Figure 6. Closed hysteresis loop*

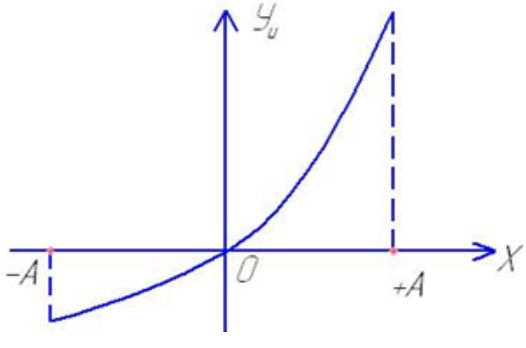

*Figure 7. Hysteresis curve*

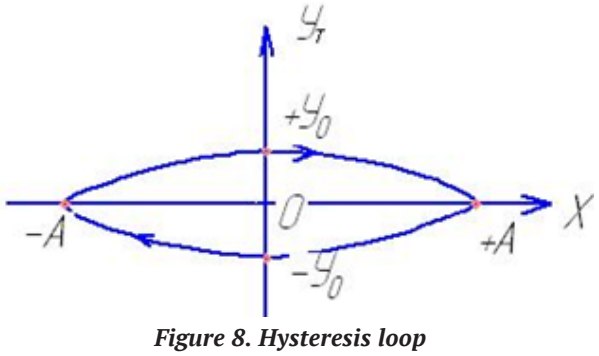

*Figure 8. Hysteresis loop*

***On harmonic linearization of hysteresis loops***

Consider a steady-state closed hysteresis loop (Fig. 6.), obtained by a harmonic law of variation of the input disturbance. In general, the shape and slope of the loop depend on the amplitude A.

$$y(x) = y_u(x) + y_T(x), \tag{12}$$

where: $y_u(x)$ is the single-digit curve of the conservative component (in Fig. 6 it is shown by a dashed line, in Fig. 7 it is shown separately), the ordinates of which are equal to the half-sum of the ordinates of the hysteresis loop at the same abscissa; $y_T(x)$ is the two-digit curve of the non-conservative component (Fig. 8), obtained by subtracting the conservative component $y_u(x)$ from the input hysteresis loop (Fig. 6).

In the case of an elastic-damping element, a material sample, and other mechanical elements, the conservative component is the elasticity curve, and the non-conservative component is the force of external or internal friction.

The component $y_T(x)$ depending on velocity $\dot{x}$ is a non-linear function that can be approximated by a linear dependence $y_T = h\dot{x}$. This approximation can be realized so that the areas of the loops corresponding to $y_T(x) = h\dot{x}$ be equal, i.e. :

$$S(A) = \pi \cdot h \cdot A^2 \cdot \omega, \tag{13}$$

where $S$ is the area of the real loop obtained as a result of the experiment; $A$ is the amplitude of the input sinusoidal signal; $\omega$ is its frequency.

From the last equation we obtain:

$$h = \frac{S(A)}{\pi \cdot A^2 \cdot \omega}, \tag{14}$$

and correspondingly:

$$y_T = \frac{S(A)}{\pi \cdot A^2 \cdot \omega} \cdot \dot{x}, \tag{15}$$

The conservative, hysteresis-free component $y_u(x)$ is approximated by a linear function:

$$y_u(x) = k(A)x, \tag{16}$$

using, for example, the method of optimal linearization of nonlinear elastic characteristics proposed by Ya.G. Panovko [17]. In the case of symmetric $y_u(x)$, the dependence $k(A)$ is calculated using the following integral:

$$k(A) = \frac{5}{A^5}\int_0^A y_u(x)x^3 dx, \tag{17}$$

In the case of asymmetric $y_u(x)$

$$k(A) = \frac{5}{2A^5}\int_{-A}^{+A} y_u(x - x_0)x^3 dx, \tag{18}$$

where: $x_1 = x + x_0$, $x_0 = \frac{A_2 - A_1}{2}$, $A = \frac{A_2 + A_1}{2}$; $A_1, A_2$ are the maximum ranges of oscillations relative to the beginning of the count; $x_0$ is the displacement of the center of oscillations.

So, we describe the hysteresis loop $y(x)$ by the following equation:

$$y(x) = k(A)x + \frac{S(A)}{\pi \cdot A^2 \cdot \omega} \cdot \dot{x}, \tag{19}$$

which takes into account the experimentally observed dependence of the slope and area of the loop on the amplitude of the input effect. We introduce the coefficient of relative hysteresis $\gamma$ for a static system in the following form

$$\gamma = \frac{S(A)}{\pi \cdot k(A) \cdot A^2}, \tag{20}$$

where: $k(A)$ is the coefficient of linearization of the loop centerline introduced above.

In accordance with this, expression (19) can be transformed:

a) in real form:

$$y = k(A)\left[x + \frac{\gamma(A)}{\omega} \cdot \dot{x}\right], \tag{21}$$

b) in complex form:

$$y = k(A)\left[1 + i\gamma(A)\right]\cdot x. \tag{22}$$

As can be seen, the form of harmonic linearization of static hysteresis characteristics remained the same as for linear systems.

**Calculation of the loops parameters obtained by the harmonic law of variation of the input signal**

As mentioned above, at harmonic law of variation of the input value of *x(t)* , the steady-state position of the hysteresis loop is reached after a certain number of cycles. The equations of the contour of a steady-state loop (Fig. 9) is written as:

$$x = \begin{cases} \Phi_1(y, c_{1n}), \dot{x} > 0; \\ \Phi_2(y, c_{2n}), \dot{x} < 0, \end{cases} \tag{23}$$

where: $C_{1n}$ , $C_{2n}$ are the values of arbitrary constants corresponding to the steady-state mode.

The loop area is calculated by the following formula:

$$S = \int_{x_0-A}^{x_0+A} [\Phi_1(y, c_{1n}) - \Phi_2(y, c_{2n})]dx. \tag{24}$$

The mid-line of the loop (Fig. 9):

$$y_{cp}(x) = \frac{\Phi_1(y, c_{1n}) + \Phi_2(y, c_{2n})}{2}, \tag{25}$$

can be approximated by a linear dependence (Fig. 9)

$$y_\Lambda(x) = kx + y_1,$$

where: *k, y-const* at a given amplitude .

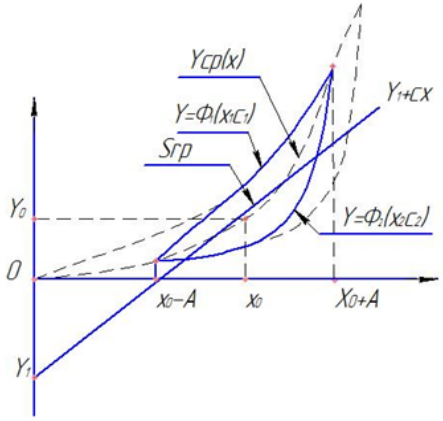


***Figure 9. Hysteresis loop***

In the case of using the least squares approximation [18], we minimize the integral:

$$I_m = \int_{x_0-A}^{x_0+A} [y_{cp}(x) - (kx + y)]^2 dx. \tag{26}$$

The result is a system of algebraic equations for calculating the parameters $k$ and $y_1$ :

$$\frac{1}{2}\frac{\partial I_m}{\partial y_1} = \int_{x_0-A}^{x_0+A} [y_{cp}(x)\cdot(kx + y)]dx = 0,$$

$$\frac{1}{2}\frac{\partial I_m}{\partial k} = \int_{x_0-A}^{x_0+A} [y_{cp}(x) - (kx + y)]xdx = 0, \tag{27}$$

or

$$S_0 y_1 + S_1 k = \int_{x_0-A}^{x_0+A} y_{cp}(x)dx,$$

$$S_1 y_1 + S_2 k = \int_{x_0-A}^{x_0+A} y_{cp}(x)xdx, \tag{28}$$

where: $S_0 = 2A,\ S_1 = 2x_0A,\ S_2 = \frac{2A}{3}\left(3x_0^2 + A^2\right)$.

The same approximation can be made by minimizing the integral:

$$I_m = \int_{x_0-A}^{x_0+A} [y_{cp}(x) - (kx + y)]^2 x^2 dx, \tag{29}$$

which provides for the so-called "weighing" along the coordinate $x$ , proposed by Ya.G. Panovko [17]. The need for such "weighing" was proven both theoretically and practically. From the minimum condition (29), we obtain a system of equations for $k$ and $y_1$ :

$$\frac{1}{2}\frac{\partial I_m}{\partial y_1} = \int_{x_0-A}^{x_0+A} [y_{cp}(x) - (kx + y_1)]x^2 dx = 0,$$

$$\frac{1}{2}\frac{\partial I_m}{\partial k} = \int_{x_0-A}^{x_0+A} [y_{cp}(x) - (kx + y)]x^3 dx = 0, \tag{30}$$

or

$$Q_0 y_1 + Q_1 k = \int_{x_0-A}^{x_0+A} y_{cp}(x)x^2 dx,$$

$$Q_1 y_1 + Q_2 k = \int_{x_0-A}^{x_0+A} y_{cp}(x)x^3 dx, \tag{31}$$

where: $Q_0 = \frac{x^3}{3},\ Q_1 = \frac{x^4}{4},\ Q_2 = \frac{x^5}{5}$.

The coefficient $\gamma$ is calculated as before by formula (20), and the coefficient $k$ is taken as a solution to equations (28) or (31).

In the case of using a computer to calculate dependencies *k(A)* and *γ(A)* it is more convenient to proceed to the discrete form of equations (28) or (31), which can be obtained by minimizing the sums:

Approximation without "weighting" along the x coordinate:

$$I_m = \sum_{i=1}^{n} [y_{cp}(x_i) - (kx_i + y_i)]^2; \tag{32}$$

Approximation with "weighting" along the *x* coordinate:

$$I_m = \sum_{i=1}^{n} [y_{cp}(x_i) - (kx_i + y_i)]^2 x_i^2. \tag{33}$$

In the first case, we get:

$$ny_1 + (\sum_{i=1}^{n} x_i)k = \sum_{i=1}^{n} y_{cp}(x_i),$$

$$(\sum_{i=1}^{n} x_i)y_1 + (\sum_{i=1}^{n} x_i^2)k = \sum_{i=1}^{n} x_i y_{cp}(x_i). \tag{34}$$

In the second case, we get:

$$(\sum_{i=1}^{n} x^2{}_i)y_1 + (\sum_{i=1}^{n} x_i^3)k = \sum_{i=1}^{n} x_i{}^2 y_{cp}(x_i),$$

$$(\sum_{i=1}^{n} x^3{}_i)y_1 + (\sum_{i=1}^{n} x_i^4)k = \sum_{i=1}^{n} x_i{}^3 y_{cp}(x_i). \tag{35}$$

Points $x_i$ are taken in the range from $x_i$-$A$ to $x_0$-$A$ with step

$\Delta x_i = \frac{2A}{\Pi}$, where $n$ is the number of steps.

By setting different values of the amplitude $A$, it is possible to obtain the dependences $k(A)$ and $\gamma(A)$, corresponding to a given operating point.

**Applications to describe hysteresis of second-order differential equations**

For a more accurate description of the hysteresis characteristics of static systems actually used in practice, in a number of cases it is preferable to use differential equations of higher order, in particular, second-order equations. Firstly, more accurate analytical description of the branches of the hysteresis loops are achieved (remember that the general solution, for example, of a linear homogeneous second-order equation with constant coefficients can contain two exponentials); secondly, the use of higher-order equations allows one to display the loop closure observed in practice for a number of static systems (in particular, systems with magnetic elements, ferroelectric capacitors, and in some cases with sources of mechanical losses) after the first cycle, which, as we saw above, is not displayed using the first-order equations. In addition, the use of higher-order differential equations allows the simulation of cyclically unstable hysteresis, when the shape and slope of the hysteresis curves can change from cycle to a number of cycles. For some systems, this process ends after a certain number of cycles (the so-called transient process in the phenomenon of hysteresis is observed, in electrical engineering in relation to magnetic elements it is called accommodation). For other systems, this process of cyclic instability of hysteresis can be observed for any length of time (this is especially characteristic for a strain of a rigid body).

For a better understanding of what has been said, we present the basic information from the theory of second-order differential equations:

$$\frac{d^2y}{dx^2} = F(x,y)\frac{dy}{dx}, \tag{36}$$

where: function $F$ is defined in domain $V$ of three-dimensional space $XOYY'$ and is continuous in it together with its partial derivatives in $y$ and $y'$ (the Cauchy conditions for the existence and uniqueness of the solution to equation (36)).

It is known that the general solution of such an equation contains two arbitrary constants $c_1$ and $c_2$:

$$y = \phi(x, c_1, c_2) \tag{37}$$

A family of integral curves $y = \phi(x, c_1, c_{2i})$, corresponds to each specific value of $C_{2i}$ $(i=1, 2, ...)$, and the shape and slope of the curves in the general case can change from family to family (Fig. 10.).

When defining a specific integral curve passing through a given point $M_0(x_0,y_0)$, the initial angle of inclination $\alpha_0\left(tg\alpha_0 = \frac{dy}{dx}G_i M_0\right)$ of the tangent to the curve at this point is also specified. It is clear that we can set this angle arbitrarily, as long as only the Cauchy problem has a unique solution. As can be seen, the general solution of the second-order differential equation reflects the fact that an infinite set of integral curves of the most diverse shapes and slopes can pass through a given point of the $XOY$ plane. At the same time, as we saw above, in the case of a first-order differential equation, when the Cauchy conditions are satisfied, only one integral curve can pass through a given point of the plane.

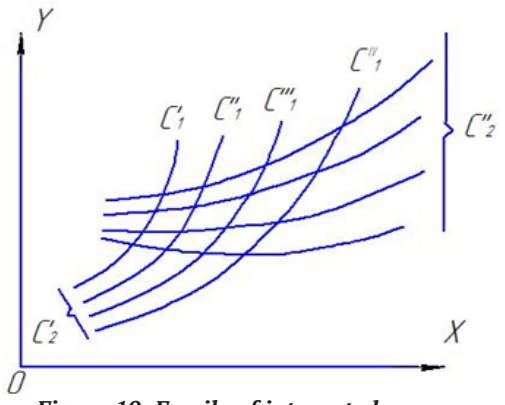


***Figure 10. Family of integrated curves***

Therefore, based on the general theory of the second-order differential equations, we describe the hysteresis characteristic with functional relations:

$$y = \begin{cases} \varphi_1(x, c_1, c_2), \dot{x} > 0; \\ \varphi_2(x, c_3, c_4), \dot{x} < 0, \end{cases} \tag{38}$$

which are solutions of differential equations:

$$\frac{d^2y}{dx^2} = \begin{cases} F_1\left(x, y, \frac{dy}{dx}\right), \dot{x} > 0; \\ F_2\left(x, y\frac{dy}{dx}\right), \dot{x} < 0. \end{cases} \tag{39}$$

In the case of computer-aided calculation of hysteresis cycles according to functional relations (38), the calculation of arbitrary constants $c_i(i=1,..4)$ can be performed in two different ways.

According to the first method, at any point of turning $A$, the coordinates $x_A, y_A$ of this point are recorded, and the tangent of the tilt angle to the corresponding curve of loading (unloading) is set. These coordinates and arbitrary values are substituted into the appropriate integral relations (the first or second expression of (38)) and its derivative, as a result of which specific values are obtained ($i$ = 1.2 or 3.4), and, hence, a specific analytical expression of the corresponding hysteresis curve.

According to the second method, the coordinates of not only the source point of turning $A$ are stored, but the coordinates of pre-source point $B$ as well. The coordinates of both points are substituted at a particular integral relation (38), as a result of which we obtain two algebraic equations to determine the corresponding arbitrary constants $c_i$. It is easy to see that in this case there is a return to the pre-source point of turn $B$ (the same situation is realized in the Rayleigh-Mazing principle).

Differential equations (39) are transformed to the following form:

$$\frac{dW}{dt} = \begin{cases} F_1(x, y, w)\frac{dx}{dt}, \dot{x} > 0; \\ F_2(x, y, w)\frac{dx}{dt}, \dot{x} < 0, \end{cases}$$
$$\frac{dy}{dt} = W\frac{dx}{dt}, \tag{40}$$

where: $W\frac{dx}{dt}$ determines the tangent tilt in the hysteresis curves field.

According to equations (40), the simulation of hysteresis characteristics of mechanical and electrical elements was conducted.

According to the well-known Rayleigh-Masing principle, an arbitrary hysteresis cycle restores the same curve *y=f(x)* at the turning points (Fig. 11) since the coordinates of the turning points are arbitrarily, and we can consider them as arbitrary constants. Let $c_1=x_A$, $c_2=y_A$ , $c_3=x_B$ , $c_4=y_B$ (see Fig. 11). In accordance with this, the equations of hysteresis characteristics are written as:

$$y=\begin{cases}-f(-x+c_1)+c_2, x>0;\\ f(x-c_3)+c_4, \dot{x}<0.\end{cases} \quad (41)$$

Differentiating relations (41) twice and eliminating arbitrary constants from the expressions obtained for the derivatives using (41), we arrive at the differential equations:

$$\frac{d^2y}{dx^2}=\begin{cases}-\theta(\frac{dy}{dx}), \dot{x}>0;\\ +\theta(\frac{dy}{dx}), \dot{x}<0,\end{cases} \quad (42)$$

where:

$$\theta=f''\left[f^{'-1}\left(\frac{dy}{dx}\right)\right]$$

Equations (40) correspond to the integral operator:

$$y=\int_0^t[\int_0^\tau R\left[x(S),y(S),w(S)\right]\dot{x}(S)dS]\dot{x}(\tau)d\tau, \quad (43)$$

where:

$$R[x(S),y(S),w(S)]=\begin{cases}F_1[x(S),y(S),w(S)], \dot{x}(S)>0;\\ F_2[x(S),y(S),w(S)], \dot{x}(S)<0.\end{cases}$$

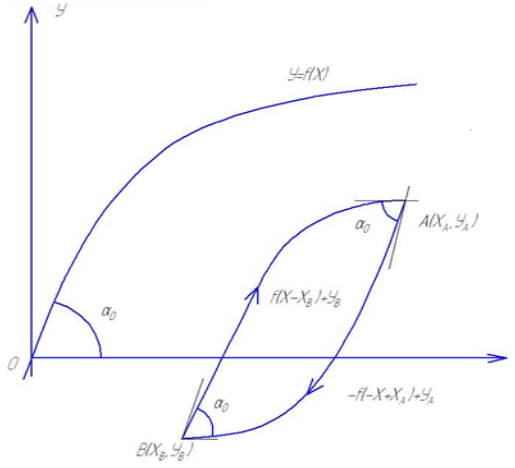


***Figure 11. Hysteresis cycle***

**Calculations**

**Plotting an unstable hysteresis cycle**

Let a monotonically increasing curve $y_0=f(x_0)$ (fragment 1) be constructed on the $X_0O_1Y_0$ plane (Fig. 12), defined on an interval *(a,b)* and having continuous first and second derivatives on this interval. The value of the first derivative at each of its points is positive and decreases monotonically with an increase in the abscissa from *a* to *b* . In particular, it can be defined either on the entire number axis (-∞ ,+∞)or on the positive semi-axis [0,+∞) . We introduce a new coordinate system *XOY* (Fig. 12) with the origin at point $O(x_0^*, y_0^*)$ at which the equation of the curve has the following form:

$$y=-y_0^*+f(x+x_0^*) \quad (44)$$

We mark with a solid line the part of this curve located in the 1st quadrant of the *XOY* plane. The selected area, transferred parallel to itself (Fig. 12, fragment 2) to the position with the origin at point $A_{k+1}(x_{k+1}, y_{k+1})$, is described by the following equation:

$$y=y_{k+1}-y_0^*+f(x+x_0^*-x_{k+1}) \quad (45)$$

The same selected part of the curve, rotated relative to point *O* , is described by the following equation:

$$y=y_0^*-f\left(-x+x_0^*\right) \quad (46)$$

and at parallel transfer to point $A_k(x_k, y_k)$ :

$$y=y_k+y_0^*+f(-x+x_0^*+x_k) \quad (47)$$

Curves (45) and (47) are used to construct a hysteresis cycle corresponding to an arbitrary continuous law of variation of the input coordinate x as a function of time $t\geq 0$.

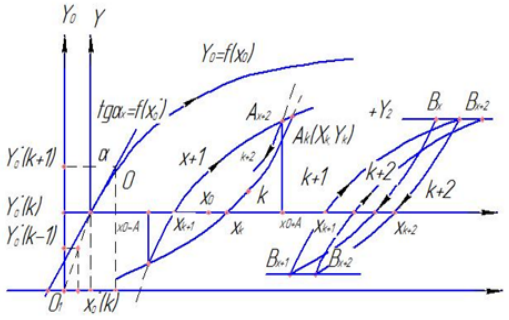


***Figure 12. Monotonically increasing curve***

We assume that at x>0 the motion of the representing point on the plane is performed along the curve (45), and at x<0 along the curve (47). At x=0 , the turning point is fixed on the *XOY* plane. In the general case of cyclically unstable hysteresis, the values of $x_0^*$ and $y_0^*=f\left(x_0^*\right)$ depend on the number of loading half-cycles *k* , i.e. are sequences of the form $x_k^*=x_0^*(k)$ $y_k^*=f(x_k)$.

As a result, the equations of the ascending and descending hysteresis curves have the following form (Fig. 12):

$$y=\begin{cases}y_{k+1}-y_{k+1}^*+f(x+x_{k+1}^*-x_{k+1}), \dot{x}>0;\\ y_k+y_k^*-f(-x+x_k^*-x_k), \dot{x}<0,\end{cases} \quad (48)$$

where: $A_k(x_k, y_k)$ , $A_{k+1}(x_{k+1}, y_{k+1})$ are the turning points at the beginning of the *k*-th (odd) and (*k* + *1*)-th half-cycles, respectively, (*k* = 1,2,3). It is easy to show by direct differentiation that $y_k'(x_k)=f'(x_k^*)$ at the k-th turning point.

Let *x* vary by some law of periodic function (which does not change the sign of the derivative in every quarter of the period) running through the values (in Fig. 12, fragment 2) within the limits $x_0-A\leq x\leq x_0+A$ .

Then, equations (48) can be rewritten as:

$$y=\begin{cases}y_{k+1}-y_{k+1}^*+f\left(x+x_{k+1}^*+A-x_0\right), \dot{x}>0;\\ y_k+y_k^*-f\left(-x+x_k^*+A+x_0\right), \dot{x}<0.\end{cases} \quad (49)$$

At the points of intersection of these curves with the abscissa, we get:

for the down-sloping curve

$$\overline{x}_k=x_0+A+x_k^*-f^{-1}\left(y_k^*+y_k\right) \quad (50)$$

At the points of intersection of these curves with the abscissa, we get:

for the down-sloping curve

$$\overline{x}_k = x_0 + A + x_k^* - f^{-1}\left(y_k^* + y_k\right) \tag{50}$$

for the upward-sloping curve

$$\overline{x}_{k+1} = x_0 + A + x_{k+1}^* - f^{-1}(y_{k+1}^* + y_{k+1})$$

As a result, the width of the loop formed at the *k*-th and (*k* + 1)-th half-cycles is:

$$b_{k,k+1} = x_k^* + x_{k+1}^* + 2A - f^{-1}\left(y_k^* + y_k\right) - f^{-1}\left(y_{k+1}^* + y_{k+1}\right) \tag{51}$$

where: $y_{k+1} = y_k + y_k^* - f(x_k^* + 2A)$

The dependence *b* on the number of cycles can be determined from experimental records of the field of curves of cyclically unstable hysteresis. Therefore, considering , the sequence can be calculated by solving the nonlinear algebraic equation (51). In addition, having a close-up record of the hysteresis field, this sequence can be found directly by superimposing and shifting over each other until the branches of the loops in the 1st and k-th half-cycles completely coincide.

According to equations (49), it is easy to distinguish the ordinates at the points $A_{k+2}$ and $A_k$, $A_{k+1}$ and $A_{k+3}$ (Fig. 12, III):

$$\begin{aligned} y_{k+2} - y_k &= -\Delta y_k^* + \Delta f_k, \\ y_{k+1} - y_{k+3} &= -\Delta y_{k+1}^* + \Delta f_{k+1}, \end{aligned} \tag{52}$$

where:

$$\begin{aligned} &\Delta y_k^* = y_{k+1}^* - y_k^*, \Delta y_{k+1}^* = y_{k+2}^* - y_{k+1}^*, \\ &\Delta f_k = f\left(x_{k+1}^* + 2A\right) - f\left(x_k^* + 2A\right), \\ &\Delta f_{k+1} = f\left(x_{k+2}^* + 2A\right) - f\left(x_{k+1}^* + 2A\right). \end{aligned}$$

Consider the behavior of the hysteresis characteristic in the following three cases:

1. The sequence $x_k^* = x_0^*(k)$ is sign-positive and monotonically increasing. By virtue of the conditions imposed on the function $y_0 = f\left(x_0\right)$ above, we obtain $\Delta y_k^* > 0$ , $\Delta y_{k+1}^* > 0$ , $\Delta y_k^* < \Delta f_k$, $\Delta y_{k+1}^* < \Delta f_{k+1}$. This means that in the first case, with the growth, the loops will narrow vertically.

2. The sequence $x_k^* = x_0^*(k)$ is sign-negative and monotonically increasing in absolute value, and $\left|x_k^*\right| < 2A$ for any *k* . It leads to $\Delta y_k^* < 0$, $\Delta y_{k+1}^* < 0$, $\Delta f_k < 0$, $\Delta f_{k+1} < 0$, $\Delta y_{k+1}^* < \Delta f_{k+1}$, $\Delta y_k^* < \Delta f_k$ .

3. Thus, in this second case, on the contrary, with the growth of *k* , the loops will expand vertically.

4. The sequence $x_k^* = x_0^*(k)$ is sign-positive and non-increasing, and for each subsequent even number *k* , the value of $x_k^*$ is greater than the corresponding value for the previous odd number. Then, according to (3.52), we obtain $y_k^* > 0$, $\Delta y_{k+1}^* < 0$, и $\Delta f^*_k > 0$, $\Delta f^*_{k+1} < 0$, and accordingly $y_{k+2} < y_k, y_{k+1} > y_{k+3}$. Thus, in the third case, the phenomenon of cyclic relaxation will be observed, which manifests itself in the downward displacement of the loop. If the difference between two adjacent values of $x^k$ decreases with increasing *k*, the cyclic relaxation will decay.

Further, let during each half-cycle the value of the output coordinate y change monotonically within the limits (in Fig. 12). Then, based on (48), we arrive at the following equations for the hysteresis curves:

$$y = \begin{cases} -y_1 - y_{k+1}^* + f\left(x + x_{k+1}^* - x_{k+1}\right), \dot{x} > 0; \\ y_2 + y_k^* - f\left(-x - x_k^* + x_k\right), \dot{x} < 0. \end{cases} \tag{53}$$

at the points of intersection with the abscissa axis we have:

For outgoing curve

$$\overline{\overline{x}}_k = x_k + x_k^* - f^{-1}\left(y_k^* + y_2\right) \tag{54}$$

for incoming curve

$$\overline{\overline{x}}_{k+1} = x_{k+1} - x_{k+1}^* + f^{-1}(y_1 + y_{k+1}'') \tag{55}$$

Accordingly, the width of the loop in the *k, (k + 1)*-th half-cycles is:

$$b_{k,k+1} = x_k - x_{k+1} + x_k^* - x_{k+1}^* - f^{-1}\left(y_k^* + y_2\right) - f^{-1}\left(y_{k+1}^* + y_1\right) \tag{56}$$

where:

$$x_{k+1} = x_k + x_k^* - f^{-1}(y_k^* + y_2 + y_1)$$

This equation can also be used to find the sequence $x_k^*$ .

Using equations (53), it is not difficult to determine the difference between the abscissas at the points $B_{k+2}$ and $B_k$ and $B_{k+1}B_{k+3}$ (Fig. 12).

$$\begin{aligned} x_{k+2} - x_k &= -\Delta x_k^* + \Delta f_k^{-1}, \\ x_{k+1} - x_{k+3} &= -\Delta x_{k+1}^* + \Delta f_{k+1}^{-1} \end{aligned} \tag{57}$$

where:

$$\begin{aligned} &\Delta x_k^* = x_{k+1}^* - x_k^*, \Delta x_{k+1}^* = x_{k+2}^* - x_{k+1}^*, \\ &\Delta x_k = \left(x_{k+1}^* - x_{k,}\right), \ \Delta x_{k+1} = \left(x_{k+1}^* - x_{k+1,}{}^*\right), \\ &\Delta f_k^{-1} = f^{-1}\left(y_{k+2}^* + y_1 + y_2\right) - f^{-1}\left(y_k^* + y_1 + y_2\right), \\ &\Delta f_{k+1}^{-1} = f^{-1}\left(y_{k+2}^* + y_1 + y_2\right) - f^{-1}\left(y_{k+1}^* + y_1 + y_2\right), \end{aligned}$$

of which, in the same order as discussed above, it follows:

1. If the sequence $x_0^*(k)$ is sign-positive and monotonically increasing, then $\Delta x_k^* > 0$, $\Delta x_{k+1}^* > 0$, $\Delta f_k^{-1} > \Delta x_k^*$, $\Delta f_{k+1}^{-1} > \Delta x_{k+1}^*$, and accordingly, $x_{k+2} > x_k$, $x_{k+3} > x_{k+1}$.

Hence, it follows that under this condition, the loop will expand horizontally with increasing *k*.

2. If the sequence $x_0^*(k)$ is sign-negative and monotonically increasing in absolute value, then $\Delta x_k^* < 0$, $\Delta x_{k+1}^* < 0$, $\Delta f_k^{-1} < \Delta x_k^*$, $\Delta f_{k+1}^{-1} < \Delta x_{k+1}^*$ and accordingly, $x_{k+2} < x_k$, $x_{k+3} < x_{k+1}$. In contrast to the previous case, this leads to a narrowing of the loop horizontally.

3. If the sequence $x_0^*(k)$ is sign-positive and non-increasing, and for each subsequent even number *k*,

the value of $x_k^*$ is greater than the corresponding value for the previous odd number, then $\Delta x_k^* > 0,\ \Delta x_{k+1}^* > 0,$ $\Delta f_k^{-1} > \Delta x_k^*,\ \Delta f_{k+1}^{-1} < \Delta x_{k+1}^*,\ x_{k+2} > x_k,\ x_{k+3} > x_{k+1},$ and the loop moves along the *OX* axis to the right, thereby demonstrating cyclic creep.

The mathematical model of hysteresis in the form (48) is suitable for studying systems with hysteresis on a computer. When using computers, it is necessary to pass from functional relations (48) to second-order differential equations. This transition is realized as follows. Since in the first functional relation (48) the coordinates $x_{k+1}$ , $y_{k+1}$ can take arbitrary values from some area (closed or non-closed) on the *XOY* plane, they can be taken as arbitrary constants $c_1$ and $c_2$, respectively. Then the first relation from (48) can be rewritten as

$$y = f(x + x_{k+1}^* - c_1) + c_2. \tag{58}$$

Differentiating this relation twice:

$$\frac{dy}{dx} = f'\left(x + x_{k+1}^* - c_1\right) = \phi\left(x + x_{k+1}^* - c_1\right),$$

$$\frac{d^2y}{dx^2} = f''\left(x + x_{k+1}^* - c_1\right) = \psi\left(x + x_k^* - c_1\right),$$

and eliminating $c_1$ , we arrive at the following differential equation:

$$\frac{d^2y}{dx^2} = \theta\left(\frac{dy}{dx}\right), \tag{59}$$

where

$$\theta = \psi\left[\varphi^{-1}\left(\frac{dy}{dx}\right)\right].$$

The initial conditions for this equation are: for

$$x = x_{k+1},\ y = y_{k+1},\ y^1 = f'(x^*_{k+1}),$$

Likewise, for the second relation from (48) we obtain an equation of the form:

$$\frac{d^2y}{dx^2} = -\theta\left(\frac{dy}{dx}\right) \tag{60}$$

where

The initial conditions for it are for:

$$x = x_k,\ y = y_k,\ y^1 = f'(x^*_k).$$

Introducing notation $W = \frac{dy}{dx}$ and using relation

$$\frac{dw}{dx} = \frac{\frac{dw}{dt}}{\frac{dx}{dt}},$$

we can write the following system of equations:

$$\frac{dw}{dt} = \begin{cases} \theta(W)\frac{dx}{dt}, \dot{x} > 0; \\ -\theta(W)\frac{dx}{dt}, \dot{x} < 0, \end{cases} \tag{61}$$

$$\frac{dy}{dt} = W\frac{dx}{dt}$$

In order to simplify the setup scheme, we will transform the variable W by the following formula:

$$W_1 = W + f_k'\ (x_k^*) \tag{62}$$

as a result, equations (61) are rewritten as:

$$\frac{dw}{dt} = \begin{cases} \theta[W_1 - f_k'\ (x_k^*)]\frac{dx}{dt}, \dot{x} > 0; \\ -\theta[W_1 - f_k'\ (x_k^*)]\frac{dx}{dt}, \dot{x} < 0, \end{cases} \tag{63}$$

$$\frac{dy}{dt} = \left[W_1 - f_k'\left(x_k^*\right)\right]\frac{dx}{dt}$$

In order to simplify the setup scheme, we will transform the variable by the following formula:

$$w_1 = w + f_x'(x_k^*), \tag{64}$$

as a result, equations (61) are rewritten as:

$$\frac{dw}{dt} = \begin{cases} \theta[W_1 - f_x'\ (x_k^*)]\frac{dx}{dt}, \dot{x} > 0; \\ -\theta[W_1 - f_x'\ (x_k^*)]\frac{dx}{dt}, \dot{x} < 0, \end{cases}$$

$$\frac{dy}{dt} = [W_1 - f_x'\ (x_k^*)]\frac{dx}{dt}.$$

**Calculation of quadrangular hysteresis**

More generally, the ascending and descending branches of the hysteresis loops can consist of several continuously conjugated arcs. Then the hysteresis characteristic in the simplest version can be represented as a set of four families of integral curves fixed on the *XOY* plane and intersecting with each other (Fig. 13), each of them is a solution to a first-order differential equation. The transition at the same sign of from a curve of one family to a curve of another family is conducted when some parameter of the curve (arc length, projection onto the coordinate axis, radius of curvature, etc.) reaches a certain value. Families of curves can be described by the following functional relationships:

$$y = \begin{cases} \Phi_1(x, c_1), \beta < \beta_1, \dot{x} > 0, \\ \Phi_2(x, c_2), \beta \geq \beta_1, \\ \Phi_3(x, c_3), \beta < \beta_2, \dot{x} < 0, \\ \Phi_4(x, c_4), \beta \geq \beta_2, \end{cases} \tag{65}$$

which are solutions of first-order differential equations of the form:

$$\frac{dy}{dt} = \begin{cases} F_1(x, y)\frac{dx}{dt}, \beta < \beta_1, \dot{x} > 0, \\ F_2(x, y)\frac{dx}{dt}, \beta \geq \beta_1, \\ F_3(x, y)\frac{dx}{dt}, \beta < \beta_2, \dot{x} < 0, \\ F_4(x, y)\frac{dx}{dt}, \beta \geq \beta_2. \end{cases} \tag{66}$$

We further consider an option of a cyclically unstable hysteresis characteristic (Fig. 13.), in which the 1st and 3rd families of integral curves are families of straight lines fixed on the XOY plane. In Fig. 14, (fragment 1), two loops were constructed in K, (K+1)-th and, (K+2), (K+3)-th half-cycles under variation of x within . The projection of the linear section onto the OX axis is used here as a parameter depending on the number of half-cycles.

In the K, (K+1)-th half-cycles, the branches of the loops are described by the following relations:

$$y = \begin{cases} a(x - x_{k+1}), x_{k+1} \leq x \leq \bar{x}_{k+1}, \\ f(x - x_{k+1}), \bar{x}_{k+1} \leq x \leq \bar{x}_{k+2}, \dot{x} > 0; \\ a(x - x_k), \bar{x}_k \leq x \leq x_{k+1}, \dot{x} < 0; \\ -f(-x + x_k), x_{k+1} \leq x \leq \bar{x}_k, \end{cases} \tag{67}$$

where: $\bar{x}_k = x_k - x_k^*,\ \bar{x}_{k+1} = x_{k+1} - x_{k+1}^*,\ x_k = x_0 + A,\ x_{k+1} = x_0 + A.$

The loop width in *K, (K + 1)*-th half-cycles is calculated by the formula:

$$b_{k,k+1} = 2A - x_k^* - \frac{1}{a}f(x_k^* + 2A) \tag{68}$$

From Fig. 14, it can be seen that in the case of a monotonically increasing sequence $x_k^* = x_0^*(k)$ , the loops will expand vertically and narrow in width, while in the case of monotonic decreasing, vice versa. The phenomenon of

cyclic relaxation will be observed if in an even half-cycle, is $x^*_{k+1}$ less than the corresponding value in an odd half-cycle.

Consider, in addition, a limited variation in y within $-y_1 \le y \le y_2$ (Fig. 14, fragment 2). The loop width is calculated by the following formula:

$$b_{k,k+1} = x^*_k + f^{-1}(y_1 + y_2 - ax^*_k) - \frac{y_1 + y_2}{a} \qquad (69)$$

In this option, it is not difficult to formulate appropriate conclusions about the behavior of loops at an increase in the number of half-cycles.

Electronic simulation of cyclically unstable hysteresis with variable linear sections is performed according to the equations $y = y_H(x)\,(\dot{x} > 0)$ in the zero half-cycle:

$$\begin{cases} y = a(x - x_k),\ \bar{x}_k < x_k \le x_k,\ \dot{x} < 0, \\ \dfrac{d^2y}{dx^2} = -\theta\left(\dfrac{dy}{dx}\right),\ x_{k+1} < x \le \bar{x}_k, \\ y = a(x - x_{k+1}),\ x_{k+1} \le x \le \bar{x}_{k+1}, \\ \dfrac{d^2y}{dx^2} = \theta\left(\dfrac{dy}{dx}\right),\ \bar{x}_{k+1} < x \le x_{k+2}, \end{cases} \qquad (70)$$

$$\bar{x}_k = x_k - x^*{}_0(k),\ \bar{x}_{k+1} = x_{k+1} - x^*{}_0(k+1)$$

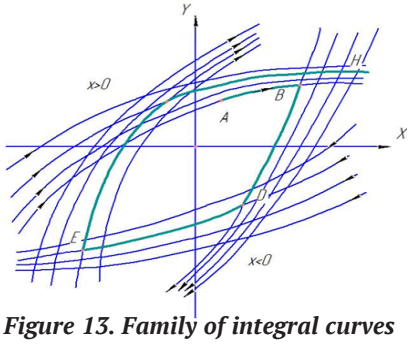


*Figure 13. Family of integral curves*

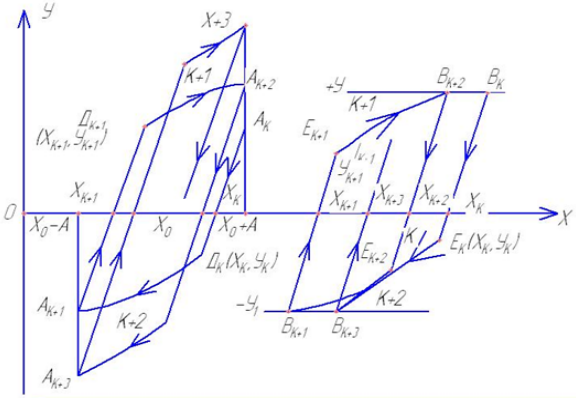


*Figure 14. Cyclically unstable hysteresis*

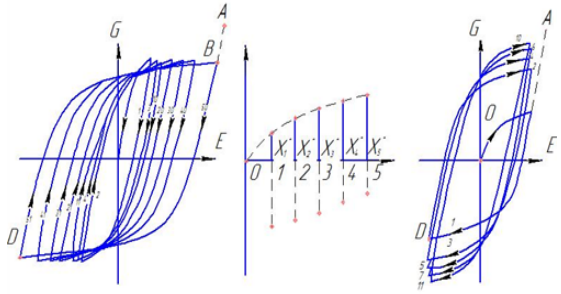


*Figure 15. Hysteresis loops*

Fig. 15 shows the experimental hysteresis characteristics of TS steel (fragment 1, soft loading) and brass 59 (fragment III, rigid loading). The superposition of the branches obtained in different half-cycles on top of each other shows that for TS steel, the BD curve can be taken as a generalized curve with a continuation up to point A (shown by a dotted line in fragment 1). If the ABD curve is sequentially superimposed on branches 41, 40, 31, 30, ... 2, 1, it can be seen how the AB section will gradually decrease. With a sufficient degree of accuracy, the AB curve can be represented as an exponential and, in accordance with (48), the hysteresis characteristic of TS steel will be described by functional relations (without considering zero half-cycle):

$$\sigma = \begin{cases} \sigma_{k+1} - \sigma^*_{k+1} + \sigma_T\left\{1 - xp[-b(\varepsilon + \varepsilon^*_{k+1} - \varepsilon_{k+1})]\right\}, \dot{\varepsilon} > 0; \\ \sigma_k + \sigma^*_k + \sigma_T\left\{1 - xp[b(\varepsilon + \varepsilon^*_k - \varepsilon_k)]\right\}, \dot{\varepsilon} < 0, \end{cases} \qquad (71)$$

where: , are the constant parameters determined by processing the hysteresis curves, for example, using the least squares method.

Since an increase in the number of half-cycles K shortens the AB curve, the sequence $\varepsilon^*_0(k)$, which acts as a projection of the AB segment onto the 0ε axis, is sign-positive and monotonically increasing (see fragment 2 in Fig. 15, solid segments). On the basis of (58), knowing that for TS steel $f(\varepsilon) = \sigma_T[1 - \exp(-b\varepsilon)]$, it is not difficult to obtain a system of differential equations, the solutions of which are relations (71).

The branches of the hysteresis characteristic of brass 59 (in Fig. 16) consists of a linear section with a slope E and a non-linear section, which is also well described by an exponential. The figure clearly shows the increase in the length of linear segment $\ell_0$ or its projection on the 0ε axis, equal to $\varepsilon^*_0$ with the increase in K. The resulting sequence $\varepsilon^*_0(k)$ is sign-negative and monotonically decreasing in absolute value (see Fig. 16, dashed segments); the fastest decrease is observed in the first three half-cycles. Based on (67) and (70), it is easy to obtain functional relations and the corresponding differential equations describing the hysteresis of brass 59.

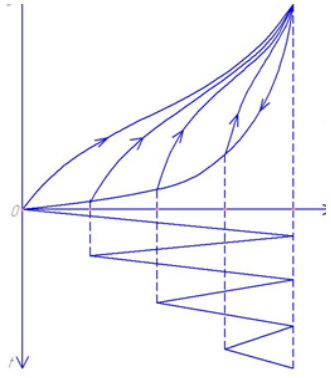

*Figure 16. Hysteresis branches*

Simulation of the hysteresis loops indicated in Fig. 15 shows good agreement between the calculated and experimental data [20, 21, 22, 23, 24, 25, 26, 27, 28, 29, 30].

**Results and discussion**

**Experimental determination of hysteresis characteristics**

Experimentally, families of curves of the hysteresis field of any static system can be obtained as follows. Let the

working field of the system on the XOУ plane be bounded by some closed curve OMPK (Fig. 16). We will excite the system from the initial point 0 by the law indicated at the bottom of Fig. 16. In this case, we register only the curves at To obtain a family of curves at , the system is excited by the law indicated below (Fig. 17). When testing static systems during every quarter cycle, the motion does not have to be linear. It is sufficient that the sign of the velocity does not change during this time (see, for example, in Fig. 17 another excitation law indicated by the dotted line).

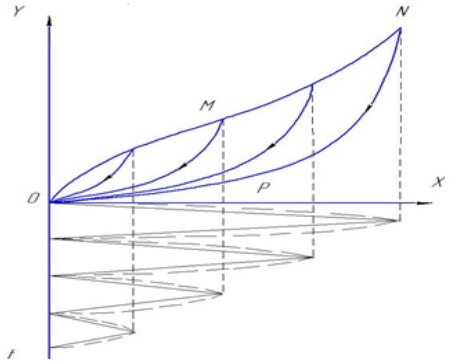


*Figure 17. Hysteresis loops*

The excitation laws shown in the figures can be obtained using special generators and tracking systems. Therefore, when testing samples of various materials, elastic damping devices and other mechanical elements of this type, the strain laws can be obtained using a servo drive, the structural diagram of which is shown in Fig. 18. Adjuster *I* provides an electrical signal $U_з(t)$, changing over time in proportion to the desired law of change in strain or force. Signal $U_з(t)$ is compared with the feedback signal $U_{oc}(t)$, coming through switch from dynamometer 6 and the internal strain $X_{об}(t)$ sensor 8 of test specimen 5. The resulting difference is the loop error signal $\Delta U_p$, which through amplifier 2 enters the control system 3 by actuator 4. The latter (of electromechanical, hydraulic or some other type) converts the loop error signal into the displacement of the machine active grip $X_з(t)$, which causes deformation of the sample, the reaction of which is perceived by the dynamometer and the loading device of the machine.

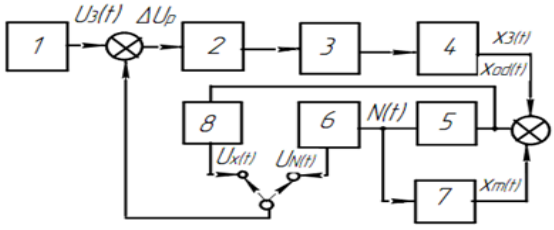


*Figure 18. Block diagram*

Under the influence of the sample, the loading device is strained, as a result of which the actual strain of the sample $X_{об}(t)$ is less than the displacement $X_з(t)$ of the active grip by the amount of machine strain $X_м(t)$ , i.e. $X_{об} = X_з(t) - X_м(t)$.

**Conclusions**

Comparatively complete information about the hysteresis field of a particular static object can be obtained using simpler sinusoidal oscillators. Therefore, in mechanical tests, we can use any mechanism (of appropriate power) of reciprocating motion with an adjustable vibration amplitude, if equipped with force and strain sensors.

In the case of using sinusoidal oscillators in different areas of the object's hysteresis field, families of hysteresis loops are recorded at different amplitudes. Comparison of the curves of hysteresis during loading and unloading, and over the entire hysteresis field will help to restore a complete pattern of the hysteresis characteristics of the object under consideration.

Mathematical models of hysteresis characteristics of static systems were developed. For a more accurate description of the hysteresis characteristics of static systems that actually occur in practice, in a number of cases, differential equations of higher order were used, in particular, second-order equations. The use of differential equations of higher order makes it possible to simulate cyclically unstable hysteresis, when the shape and slope of the hysteresis curves can change from cycle to a number of cycles. For some systems, this process ends after a certain number of cycles, for other systems, this process of cyclic instability of hysteresis can be observed for any length of time.

**References**

1. Bakhvalov, N.S., 1975. Numerical methods (analysis, algebra, ordinary differential equations). Moscow: Nauka.
2. Neimark, Yu.I., Kogan, N.Ya., Savelyev, V.P. 1985. Dynamic models of control theory. Moscow: Nauka.
3. Bu, R. 1969. Mathematical model of hysteresis. Application to an oscillating circuit with a saturable trottle. Proceedings of the V International Conference on Nonlinear Oscillations. 4, 100.
4. Krasnoselsky, M.A., Pokrovsky, A.V., 1976. Modeling of converters with hysteresis by continuous relay systems. DAN USSR. 227 (3), Pp.547-550.
5. Lebedev, A.B. 1999. Amplitude-dependent elastic modulus defect in basic models of dislocation hysteresis. Solid State Physics, 41 (7), P.p 1214-1222.
6. Lukichev, A.A., Il'ina, V.V., 2011. A simple mathematical model of the hysteresis loop for nonlinear materials. Bulletin of the Samara Scientific Center of the Russian Academy of Sciences, 13 (4), P.p 39-44.
7. Grechukhin, V.N., 2005. Mathematical description of the hysteresis loop. "Bulletin of ISEU", 1.
8. Terleev, V.V., Nikonorov, A.O., Ginevsky, R.S., Lazarev, V.A., Togo, I., Topaj, A.G., Moiseev, K.G., Pavlova, V.A., Layshev, K.A., Arkhipov, M.V., Melnichuk, A.Yu., Dunaieva, I.A., Mirschel, W. 2018. Hysteresis of the soil water-retention capacity: estimating the scanning branches. Engineering and construction journal, 1. doi: 10.18720/MCE.77.13
9. An-Nan Zhou, 2013. A contact angle-dependent hysteresis model for soil–water retention behaviour, Computers and Geotechnics. 49, Pp.36-42.

10. Poria S. Saberi, Günther Meschke, 2021. A hysteresis model for the unfrozen liquid content in freezing porous media, Computers and Geotechnics. 134, 104048.
11. He Chen, Ke Chen, Minghui Yang, 2020. A new hysteresis model of the water retention curve based on pore expansion and contraction, Computers and Geotechnics. 121, 103482.
12. Ran Hu, Yi-Feng Chen, Hui-Hai Liu, Chuang-Bing Zhou, 2015. A coupled stress–strain and hydraulic hysteresis model for unsaturated soils: Thermodynamic analysis and model evaluation, Computers and Geotechnics. 63, Pp. 159-170.
13. Taborda, D.M.G., Potts, D.M., Zdravković, L. 2016. On the assessment of energy dissipated through hysteresis in finite element analysis, Computers and Geotechnics. 71, Pp.180-194.
14. Li, X.S., 2005. Modelling of hysteresis response for arbitrary wetting/drying paths, Computers and Geotechnics. 32(2), Pp. 133-137.
15. Moghaddasi, H., Shahbodagh, B., Khalili, N., 2021. A bounding surface plasticity model for unsaturated structured soils, Computers and Geotechnics. 138, 104313.
16. Guoqing Cai, Bowen Han, Annan Zhou, Jian Li, Chenggang Zhao, 2022. Fractional-order bounding surface model for unsaturated soils under cyclic loading, Computers and Geotechnics. 141, 104529.
17. Panovko, Ya.G., 1960. Internal friction at oscillations of elastic systems. Fizmatgiz, Moscow.
18. Goncharov, V.A. 2009. Optimization methods. Higher education, Moscow.
19. Bakhvalov, N.S., Zhidkov, N.P., Kobelkov, G.M. 1987. Numerical methods. Moscow. Nauka.
20. Shahbodagh-Khan, B., Khalili, N., 2015. Alipour Esgandani, G., 2015. A numerical model for nonlinear large deformation dynamic analysis of unsaturated porous media including hydraulic hysteresis. Computers and Geotechnics. 69, P.p 411-423.
21. Chao Yang, Daichao Sheng, John P. Carter, 2012. Effect of hydraulic hysteresis on seepage analysis for unsaturated soils. Computers and Geotechnics. 41, Pp. 36-56.
22. Arash Azizi, Cristina Jommi, Guido Musso, 2017. A water retention model accounting for the hysteresis induced by hydraulic and mechanical wetting-drying cycles. Computers and Geotechnics. 87, Pp.86-98.
23. Dorival M. Pedroso, David J. Williams, 2010. A novel approach for modelling soil–water characteristic curves with hysteresis. Computers and Geotechnics. 37(3), Pp. 374-380.
24. Ran Hu, Jia-Min Hong, Yi-Feng Chen, Chuang-Bing Zhou, 2018. Hydraulic hysteresis effects on the coupled flow–deformation processes in unsaturated soils: Numerical formulation and slope stability analysis. Applied Mathematical Modelling. 54, Pp. 221-245.
25. Michael Ruderman, 2016. State-space formulation of scalar Preisach hysteresis model for rapid computation in time domain. Applied Mathematical Modelling. 40(4), Pp. 3451-3458.
26. Jozef Vörös, 2015. Identification of nonlinear cascade systems with output hysteresis based on the key term separation principle. Applied Mathematical Modelling. 39(18), Pp. 5531-5539.
27. Alessia Berti, Claudio Giorgi, Elena Vuk, 2015. Hysteresis and temperature-induced transitions in ferromagnetic materials. Applied Mathematical Modelling. 39(2), Pp. 820-837.
28. Zijian Zhang and Yangyang Dong, 2019. Asymmetrically Dynamic Coupling Hysteresis in Piezoelectric Actuators: Modeling Identification and Experimental Assessments. International Journal of Applied Mechanics. 11(05), 1950051.
29. Longbiao Li, 2015. Micromechanical Modeling for Fatigue Hysteresis Loops of Fiber-Reinforced Ceramic–Matrix Composies Under Multiple Loading Stress Levels. International Journal of Applied Mechanics. 07(06), 1550087.
30. B.A.Khudayarov, F.Zh.Turaev Mathematical Simulation of Nonlinear Oscillations of Viscoelastic Pipelines Conveying Fluid, Applied Mathematical Modelling 66 (2019), Pp. 662-679.
31. B.A.Khudayarov, Kh.M.Komilova, Vibration and dynamic stability of composite pipelines conveying a two-phase fluid flows, Engineering Failure Analysis 104 (2019), Pp. 500-512.
32. B.A.Khudayarov, Kh.M.Komilova and F.Zh.Turaev, Numerical Simulation of Vibration of Composite Pipelines Conveying Pulsating Fluid, International Journal of Applied Mechanics 11(9), 2019, 1950090.
33. B.A.Khudayarov, F.Zh.Turaev Numerical simulation of nonlinear oscillations of a viscoelastic pipeline with fluid, Vestnik of Tomsk State University. Mathematics and mechanics 5(43) (2016) Pp. 90-98.
34. B.A.Khudayarov, Kh.M.Komilova, F.Zh.Turaev, The effect of two-parameter of Pasternak foundations on the oscillations of composite pipelines conveying gas-containing fluids, International Jurnal of Pressure Vessels and Piping, 176 (2019) 103946.